GEOPHYSICAL RESEARCH LETTERS, VOL. 34, L13705, doi:10.1029/2007GL030288, 2007

A new dynamical mechanism for major climate shifts

Anastasios A. Tsonis,[1] Kyle Swanson,[1] and Sergey Kravtsov[1]

Received 5 April 2007; revised 16 May 2007; accepted 15 June 2007; published 12 July 2007.

[1] We construct a network of observed climate indices in the period 1900–2000 and investigate their collective behavior. The results indicate that this network synchronized several times in this period. We find that in those cases where the synchronous state was followed by a steady increase in the coupling strength between the indices, the synchronous state was destroyed, after which a new climate state emerged. These shifts are associated with significant changes in global temperature trend and in ENSO variability. The latest such event is known as the great climate shift of the 1970s. We also find the evidence for such type of behavior in two climate simulations using a state-of-the-art model. This is the first time that this mechanism, which appears consistent with the theory of synchronized chaos, is discovered in a physical system of the size and complexity of the climate system. **Citation:** Tsonis, A. A., K. Swanson, and S. Kravtsov (2007), A new dynamical mechanism for major climate shifts, *Geophys. Res. Lett.*, *34*, L13705, doi:10.1029/2007GL030288.

1. Introduction

[2] One of the most important and mysterious events in recent climate history is the climate shift in the mid-1970s [*Graham*, 1994]. In the northern hemisphere 500-hPa atmospheric flow the shift manifested itself as a collapse of a persistent wave-3 anomaly pattern and the emergence of a strong wave-2 pattern. The shift was accompanied by sea-surface temperature (SST) cooling in the central Pacific and warming off the coast of western North America [*Miller et al.*, 1994]. The shift brought sweeping long-range changes in the climate of northern hemisphere. Incidentally, after "the dust settled," a new long era of frequent El Niños superimposed on a sharp global temperature increase begun. While several possible triggers for the shift have been suggested and investigated [*Graham*, 1994; *Miller et al.*, 1994; *Graham et al.*, 1994], the actual physical mechanism that led to this shift is not known. Understanding the dynamics of such phenomena is essential for our ability to make useful prediction of climate change. A major obstacle to this understanding is the extreme complexity of the climate system, which makes it difficult to disentangle causal connections leading to the observed climate behavior. Here we present a novel approach, which reveals an important new mechanism in climate dynamics and explains several aspects of the observed climate variability in the late 20th century.

2. Methods and Results From Observations

[3] First we construct a network from four major climate indices. The network approach to complex systems is a rapidly developing methodology, which has proven to be useful in analyzing such systems' behavior [*Albert and Barabasi*, 2002; *Strogatz*, 2001]. In this approach, a complex system is presented as a set of connected nodes. The collective behavior of all the nodes and links (the topology of the network) describes the dynamics of the system and offers new ways to investigate its properties. The indices represent the Pacific Decadal Oscillation (PDO), the North Atlantic Oscillation (NAO), the El Niño/Southern Oscillation (ENSO), and the North Pacific Oscillation (NPO) [*Barnston and Livezey*, 1987; *Hurrell*, 1995; *Mantua et al.*, 1997; *Trenberth and Hurrell*, 1994]. These indices represent regional but dominant modes of climate variability, with time scales ranging from months to decades. NAO and NPO are the leading modes of surface pressure variability in northern Atlantic and Pacific Oceans, respectively, the PDO is the leading mode of SST variability in the northern Pacific and ENSO is a major signal in the tropics. Together these four modes capture the essence of climate variability in the northern hemisphere. Each of these modes involves different mechanisms over different geographical regions. Thus, we treat them as nonlinear sub-systems of the grand climate system exhibiting complex dynamics. Indeed, some of their dynamics have been adequately explored and explained by simplified models, which represent subsets of the complete climate system and which are governed by their own dynamics [*Elsner and Tsonis*, 1993; *Schneider et al.*, 2002; *Marshall et al.*, 2001; *Suarez and Schopf*, 1998]. For example, ENSO has been modeled by a simplified delayed oscillator in which the slower adjustment timescales of the ocean supply the system with the memory essential to oscillation. Monthly-mean values in the interval 1900–2000 are available for all indices (http://jisao.washington.edu/datasets, for NAO, PDO and El Nino, http://www.cgd.ucar.edu/cas.jhurrell/indices.html, for NPO).

[4] In our approach, the four climate indices are assumed to form a network of interacting nodes. A commonly used measure to describe variations in the network's topology is the mean distance $d(t)$ [*Onnela et al.*, 2005].

$$d(t) = \frac{2}{N(N-1)} \sum_{d_{ij}^t \epsilon D^t} d_{ij}^t \qquad (1)$$

Here t denotes the time in the middle of a sliding window of width Δt, $N = 4$; $i, j = 1,\ldots, N$, and $d_{ij}^t = \sqrt{2\left(1 - |\rho_{ij}^t|\right)}$, where ρ_{ij}^t is the cross-correlation coefficient between nodes i

[1]Department of Mathematical Sciences, Atmospheric Sciences Group, University of Wisconsin-Milwaukee, Milwaukee, Wisconsin, USA.

0094-8276/07/2007GL030288$05.00

and j in the interval [t − Δt/2, t + Δt/2], and D^t is the NxN distance matrix. The sum is taken over the upper triangular part (or the distinct elements of D^t). The above formula uses the absolute value of the correlation coefficient because the choice of sign of indices is arbitrary. The distance can be thought as the average correlation between all possible pairs of nodes and is interpreted as a measure of the synchronization of the network's components. Synchronization between nonlinear (chaotic) oscillators occurs when their corresponding signals converge to a common, albeit irregular, signal. In this case, the signals are identical and their cross-correlation is maximized. Thus, a distance of zero corresponds to a complete synchronization and a distance of $\sqrt{2}$ signifies a set of uncorrelated nodes.

[5] Figure 1a shows the distance as a function of time for a window length of Δt = 11 years, with tick marks corresponding to the year in the middle of the window. The correlations (and thus distance values for each year) were computed based on the annual-mean indices constructed by averaging the monthly indices over the period of November–March. The dashed line parallel to the time axis in Figure 1a represents the 95% significance level associated with the null hypothesis that the observed indices are sampled from a population of a 4-dimensional AR-1 process driven by a spatially (cross-index) correlated Gaussian noise; the parameters of the AR-1 model and the covariance matrix of the noise are derived from the full time series of the observed indices. This test assumes that the variations of the distance with time seen in Figure 1a are due to sampling associated with a finite-length (11-yr) sliding window used to compute the local distance values. Retaining overall cross-correlations in constructing the surrogates makes this test very stringent. Nevertheless, we still find five times (1910s, 1920s, 1930s, 1950s, and 1970s) when distance variations fall below the 95% significance level. We therefore conclude that these features are not likely to be due to sampling limitations but they represent statistically significant synchronization events. Note that the window length used in Figure 1a is a compromise between being long enough to estimate correlations but not too long to "dilute" transitions. Nevertheless, the observed synchronizations are insensitive to the window size in a wide range of 7 yr $\leq \Delta t \leq$ 15 yr.

[6] An important aspect in the theory of synchronization between coupled nonlinear oscillators is coupling strength. It is vital to note that synchronization and coupling are not interchangeable; for example, it is trivial to construct a pair of coupled simple harmonic oscillators whose displacements are in quadrature (and hence perfectly uncorrelated), but whose phases are strongly coupled [*Vanassche et al.*, 2003]. As such, coupling is best measured by how strongly the phases of different modes of variability are linked. The theory of synchronized chaos predicts that in many cases when such systems synchronize, an increase in coupling between the oscillators may destroy the synchronous state and alter the system's behavior [*Heagy et al.*, 1995; *Pecora et al.*, 1997]. In view of the results above, the question thus arises as to how the synchronization events in Figure 1a relate to coupling strength between the nodes. It should be noted that in this study we are interested in the complete synchronization among the nodes, rather than weaker types of synchronization, such as phase synchronization [*Boccaletti et al.*, 2002; *Maraun and Kurths*, 2005] or clustered synchronization [*Zhou and Kurths*, 2006], which are also important in climate interactions.

[7] For our purposes here, if future changes in the phase between pairs of climate modes can be readily predicted using only information about the current phase, those modes may be considered strongly coupled [*Smirnov and Bezruchko*, 2003]. Here we chose to study coupling using symbolic dynamics. For any given time series point, we can define a symbolic phase by examining the relationship between that point and its nearest two neighbors in time. As shown in Figure 2, if the 3 points are sequentially increasing, we can assign to the middle point a phase of 0, while if they are sequentially decreasing, a phase of π. Intermediate values then follow. Notice that this procedure is totally non-parametric, as it does not compare the actual values of the points aside from whether a point is larger or smaller than its neighbors. The advantage of this approach is that it is blind to ultra-low frequency variability, i.e., decadal scale and longer. Use of symbolic dynamics is appropriate in this case, as we are primarily interested in changes in the synchronicity and coupling of climate modes over decadal time scales. The symbolic phase ϕ^j_n is constructed separately for the four climate indices, where j denotes the index and n the year. The phases for a given year n are represented by the complex phase vector $\vec{Z}_n$ with elements $Z^j_n = \exp(i\ \phi^j_n)$. The predictability of this phase vector from year to year provides a measure of the coupling and is determined using the least squares estimator

$$\vec{Z}^{est}_{n+1} = \mathbf{M}\vec{Z}_n \tag{2}$$

where $\mathbf{M} = [\mathbf{Z}_+\ \mathbf{Z}^T]\ [\mathbf{Z}\ \mathbf{Z}^T]^{-1}$ is the least squares predictor. Here $\mathbf{Z}$ and $\mathbf{Z}_+$ are the matrices whose columns are the vectors $\vec{Z}_n$ and $\vec{Z}_{n+1}$, respectively, constructed using all years. A measure of the coupling then is simply $\|\vec{Z}^{est}_{n+1} - \vec{Z}_{n+1}\|^2$, where strong coupling is associated with small values of this quantity, i.e., good phase prediction.

[8] This quantity is plotted in Figure 1b. Figures 1c and 1d show the global surface temperature (http://data.giss.nasa.gov/gistemp/) and El Nino index in our period. Figure 1 tells a remarkable story. First let's consider the event in 1910s. The network synchronizes at about 1910. At that time the coupling strength begins to increase. Eventually the network comes out of the synchronous state sometime in late 1912 early 1913 (marked by the left vertical line). The destruction of the synchronous state coincides with the beginning of a sharp global temperature increase and a tendency for more frequent and strong El Nino events. The network enters a new synchronization state in the early 1920s but this is not followed by an increase in coupling strength. In this case no major shifts are observed in the behavior of global temperature and ENSO. Then the system enters a new synchronization state in the early 1930. Initially this state was followed by a decrease in coupling strength and again no major shifts are observed. However, in the early 1940s the still present synchronous state is subjected to an increase in coupling strength, which soon destroys it (at the time indicated by the middle vertical line). As the synchronous state is destroyed, a new shift in both temperature trend and ENSO variability is observed. The global temperature enters a cooling regime and El Ninos

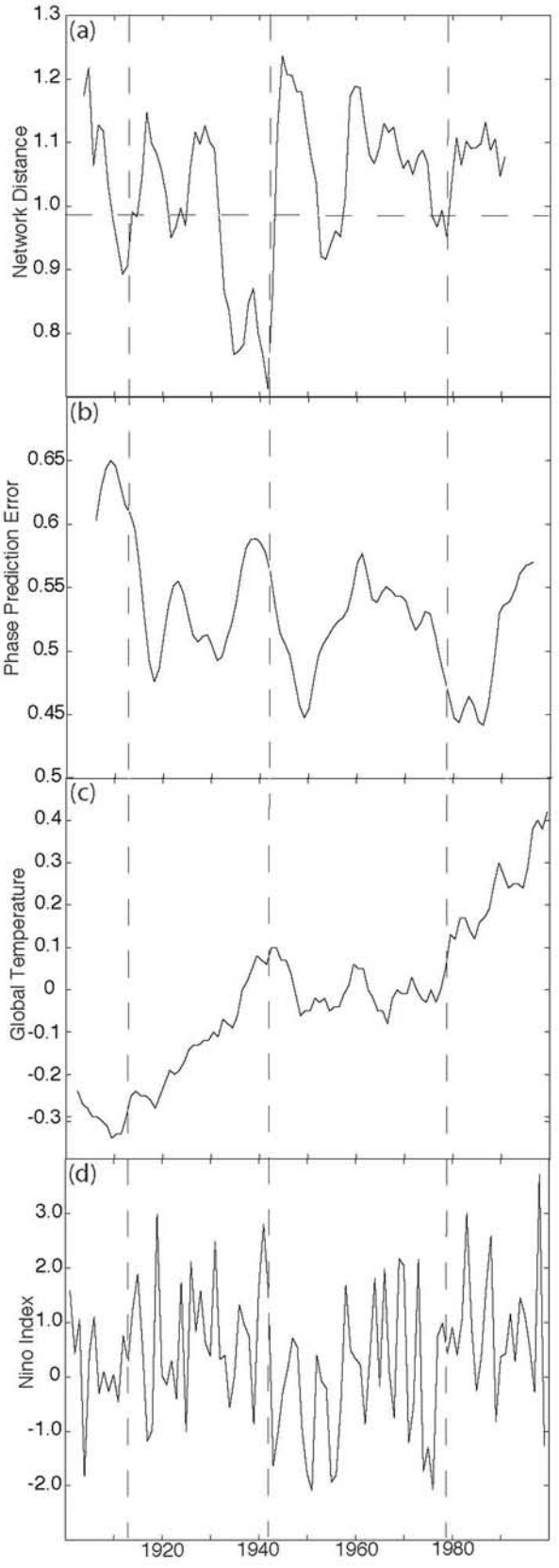

Figure 2. The six states for the symbolic phase construction. The points in each triplet correspond to three consecutive points in a time series, and their relative vertical positions to each other indicate their respective values.

become much less frequent and weaker. The network synchronizes again in 1950. This state is followed by a decrease in coupling strength and, as was the case in 1920s no major shifts occur. Finally, the network synchronizes again in the mid 1970s. This state is followed by an increase in coupling strength and incredibly, as in the cases of 1910 and 1940, synchronization is destroyed (at the time marked by the right vertical line) and then climate shifts again. The global temperature enters a warming regime and El Ninos become frequent and strong. The fact that around 1910, 1940, and in the late 1970s climate shifted to a completely new state indicates that synchronization followed by an increase in coupling between the modes leads to the destruction of the synchronous state and the emergence of a new state.

3. Model Results

[9] According to the theory of synchronized chaos such shifts in systems of nonlinear coupled oscillators are caused by bifurcations as the coupling parameter changes. Thus, the coupling strength acts as an external parameter modifying the system. In our case the coupling strength is estimated from the data and thus it is not clear whether its variability is dictated by some external forcing acting on the system or it is intrinsic. In order to further investigate this issue we considered two simulations of a state-of-the-art coupled ocean/atmosphere model. The particular model we examine here is the GFDL CM2.1 coupled ocean/atmosphere model [*GFDL CM2.1 development team*, 2006]. The first simulation is an 1860 pre-industrial conditions 500-year control run and the second is the SRESA1B, which is a "business as usual" scenario with CO_2 levels stabilizing at 720 ppmv at the close of the 21st century [*Intergovernmental Panel on Climate Change*, 2001]. From these model outputs we construct the same indices and their network.

[10] Figure 3 shows information analogous to Figure 1 but for the 2nd century of the control run. The 1st century is

Figure 1. (a) The distance (see definition in text) of a network consisting of four observed major climate modes as a function of time. This distance is an indication of synchronization between the modes with smaller distance implying larger synchronization. The parallel dashed line represents the 95% significance level associated with a null hypothesis of spatially correlated red noise. (b) Coupling strength between the four modes as a function of time. (c) The global surface temperature record. (d) Global-SST ENSO index. The vertical lines indicate the time when the network goes out of synchronization for those cases where synchronization is followed by a coupling strength increase.

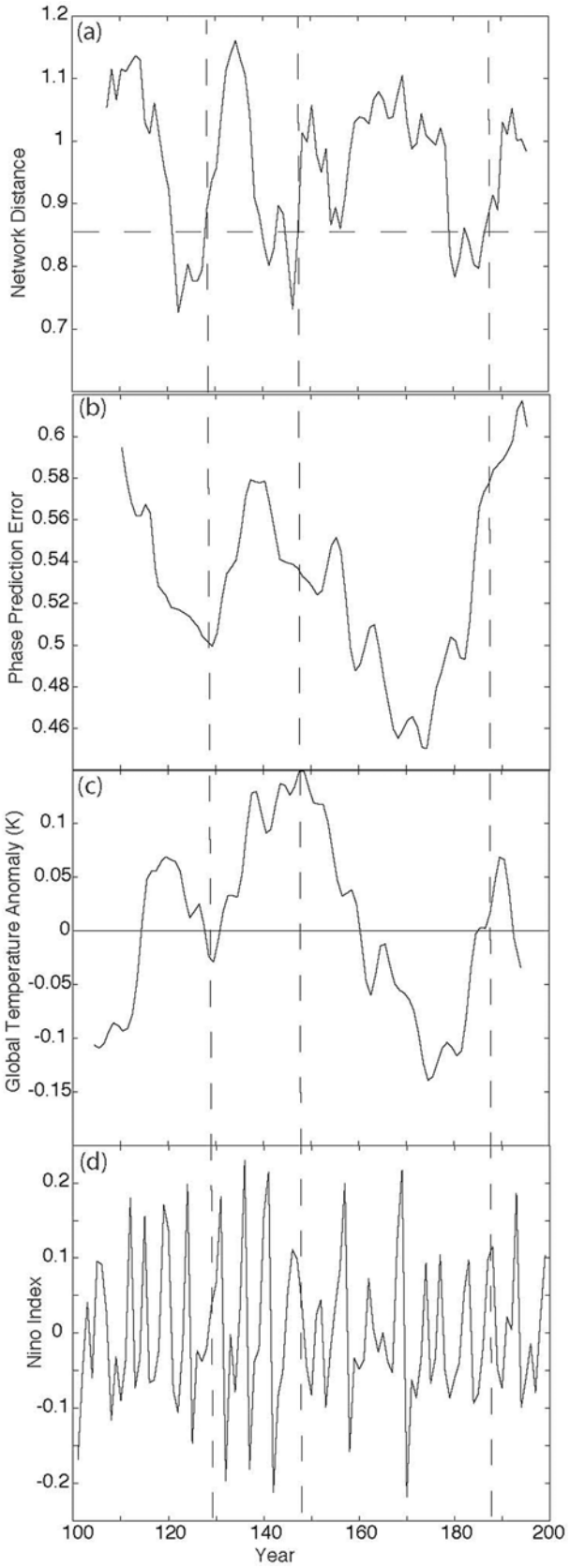

Figure 3. Same as Figure 1 but for a control run of GFDL CM2.1 model with 1860 pre-industrial conditions. See text for discussion.

not considered to avoid the effect of transients. In the other centuries the frequency of synchronization has decrease to one event per century. The general mechanism observed in the actual data is observed here as well. We observe three synchronization events, around years 120–130, years 139–148, and years 180–188. Once in place, the first two events are followed by an increase in coupling strength which eventually destroys the synchronous states. This marks a shift in both the global temperature trend and ENSO variability. The third event is not followed by a coupling strength increase and when it terminates there are no noticeable shifts. There is a temperature (but not an ENSO variability) shift in the mid 170s which is not associated with this mechanism.

[11] Figure 4 is analogous to Figure 1 but for the 21st century simulation, with the exception that the greenhouse gases radiative trend of 2°C/century in global temperature (Figure 4c) is removed to better isolate internal shifts in behavior. In this simulation we observe two synchronization events, one in years 2027–2032 and another in years 2065–2072 (with an interruption in the middle). During both events the coupling strength increases until the synchronous states are destroyed. Here again these events are associated with marked temperature trend and ENSO variability shifts.

[12] We thus find this mechanism present in observations and in model simulations. The fact that this mechanism is present in the control run will indicate that the shifts are not caused by some kind of bifurcation (which will require external influences) but rather it is an intrinsic property of the climate system. The mechanism of synchronization followed by an increase in coupling leading to a change in climate behavior seems to be rather robust. For example, it remains in a larger network that includes PNA, WP, and TNA possibly because of their regional ties to the four major modes used here. Thus, larger networks may not offer additional information Note, however, that if new nodes do not represent significant modes of variability their addition may mask the mechanism. In addition, we identify the mechanism in networks with only three nodes as long as they represent all three major regions (tropics, north Pacific and north Atlantic; i.e. ENSO, NAO and either PDO or NPO). It appears that the key to this mechanism is not the inclusion of many nodes but the interplay of the (few) most dominant modes of climate variability in the northern hemisphere.

4. Conclusions

[13] The above observational and modeling results suggest the following intrinsic mechanism of the climate system leading to major climate shifts. First, the major climate modes tend to synchronize at some coupling strength. When this synchronous state is followed by an increase in the coupling strength, the network's synchronous state is destroyed and after that climate emerges in a new state. The whole event marks a significant shift in climate. It is interesting to speculate on the climate shift after the 1970s event. The standard explanation for the post 1970s warming is that the radiative effect of greenhouse gases overcame shortwave reflection effects due to aerosols [*Mann and Emanuel*, 2006]. However, comparison of the 2035 event in the 21st century simulation and the 1910s event

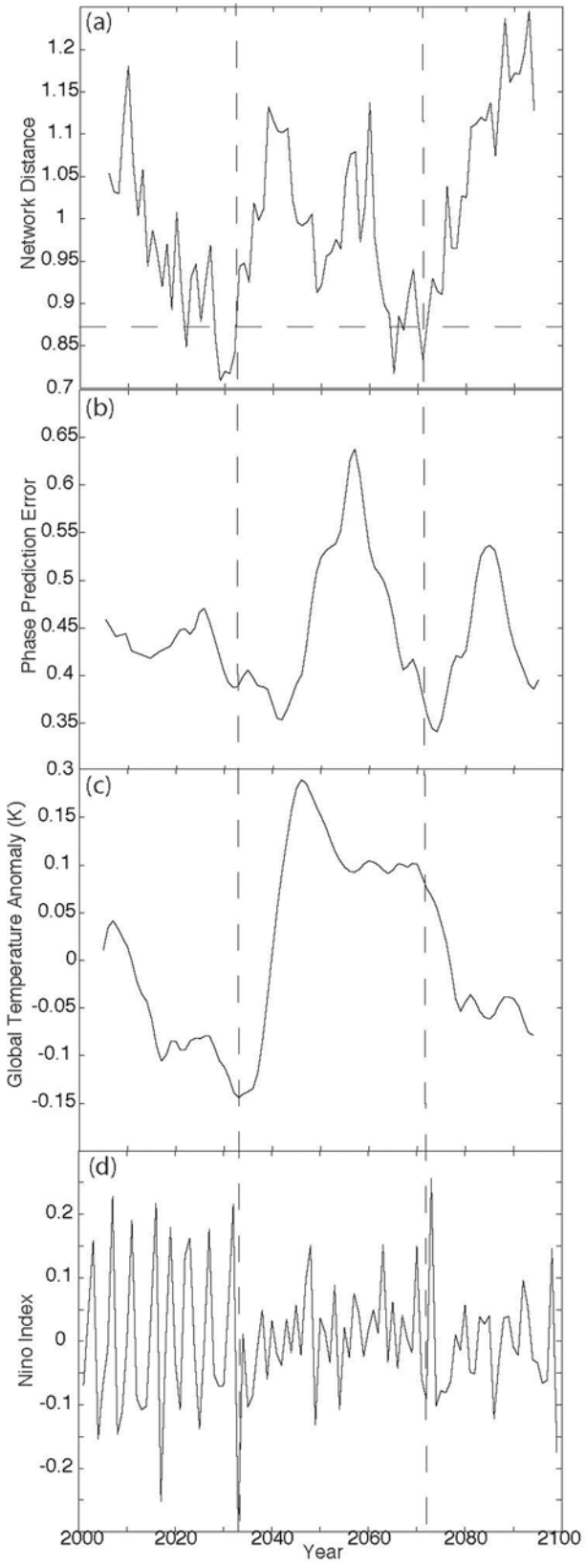

Figure 4. Same as Figure 1 but for the GFDL CM2.1 SRESA1B simulation. See text for discussion.

in the observations with this event, suggests an alternative hypothesis, namely that the climate shifted after the 1970s event to a different state of a warmer climate, which may be superimposed on an anthropogenic warming trend.

[14] **Acknowledgments.** We thank J. B. Elsner and three reviewers for their critical comments and suggestions. A.A.T. and K.L.S. are supported by NSF grant ATM-0438612; S.K. is supported by DOE grant DE-FG-03-01ER63260 and by NASA grant NNG-06-AG66G-1.

References

Albert, R., and A.-L. Barabasi (2002), Statistical mechanics of complex networks, *Rev. Mod. Phys.*, *74*, 47–101.

Barnston, A. G., and R. E. Livezey (1987), Classification, seasonality, and persistence of low-frequency atmospheric circulation patterns, *Mon. Weather Rev.*, *115*, 1083–1126.

Boccaletti, S., J. Kurths, G. Osipov, D. J. Valladares, and C. S. Zhou (2002), The synchronization of chaotic systems, *Phys. Rep.*, *366*, 1–101.

Elsner, J. B., and A. A. Tsonis (1993), Nonlinear dynamics established in the ENSO, *Geophys. Res. Lett.*, *20*, 213–216.

GFDL CM2.1 development team (2006), GFDL's CM2 global coupled climate models, parts 1–4, *J. Clim.*, *19*, 643–740.

Graham, N. E. (1994), Decadal scale variability in the tropical and North Pacific during the 1970s and 1980s: Observations and model results, *Clim. Dyn.*, *10*, 135–162.

Graham, N. E., T. P. Barnett, R. Wilde, M. Ponater, and S. Schubert (1994), On the roles of tropical and mid-latitude SSTs in forcing interannual to interdecadal variability in the winter Northern Hemisphere circulation, *J. Clim.*, *7*, 1500–1515.

Heagy, J. F., L. M. Pecora, and T. L. Carroll (1995), Short wavelength bifurcations and size instabilities in coupled oscillator systems, *Phys. Rev. Lett.*, *74*, 4185–4188.

Hurrell, J. W. (1995), Decadal trends in the North Atlantic oscillation regional temperature and precipitation, *Science*, *269*, 676–679.

Intergovernmental Panel on Climate Change (2001), *Climate Change 2001: The Scientific Basis. Contribution of Working Group I to the Third Assessment Report of the Intergovernmental Panel on Climate Change*, edited by J. T. Houghton et al., Cambridge Univ. Press, New York.

Mann, M. E., and K. A. Emanuel (2006), Atlantic hurricane trends linked to climate change, *Eos Trans. AGU*, *87*, 233.

Mantua, N. J., S. R. Hare, Y. Zhang, J. M. Wallace, and R. C. Francis (1997), A Pacific interdecadal climate oscillation with impacts on salmon production, *Bull. Am. Meteorol. Soc.*, *78*, 1069–1079.

Maraun, D., and J. Kurths (2005), Epochs of phase coherence between El Niño/Southern Oscillation and Indian monsoon, *Geophys. Res. Lett.*, *32*, L15709, doi:10.1029/2005GL023225.

Marshall, J., et al. (2001), North Atlantic climate variability: Phenomena, impacts and mechanisms, *Int. J. Climatol.*, *21*, 1863–1898.

Miller, A. J., D. R. Cayan, T. P. Barnett, N. E. Craham, and J. M. Oberhuber (1994), The 1976–77 climate shift of the Pacific Ocean, *Oceanography*, *7*, 21–26.

Onnela, J.-P., J. Saramaki, J. Kertesz, and K. Kaski (2005), Intensity and coherence of motifs in weighted complex networks, *Phys. Rev. E*, *71*, 065103.

Pecora, L. M., T. L. Carroll, G. A. Johnson, and D. J. Mar (1997), Fundamentals of synchronization in chaotic systems, concepts, and applications, *Chaos*, *7*, 520–543.

Schneider, N., A. J. Miller, and D. W. Pierce (2002), Anatomy of North Pacific decadal variability, *J. Clim.*, *15*, 586–605.

Smirnov, D. A. (2003), Estimation of interaction strength and direction from short and noisy time series, *Phys. Rev. E*, *68*, 046209.

Strogatz, S. H. (2001), Exploring complex networks, *Nature*, *410*, 268–276.

Suarez, M. J., and P. S. Schopf (1998), A delayed action oscillator for ENSO, *J. Atmos. Sci.*, *45*, 549–566.

Trenberth, K. E., and J. W. Hurrell (1994), Decadal atmospheric-ocean variations in the Pacific, *Clim. Dyn.*, *9*, 303–319.

Vanassche, P., G. G. E. Gielen, and W. Sansen (2003), Behavioral modeling of (coupled) harmonic oscillators, *IEEE Trans. Comput. Aided Design Integr. Circuits Syst.*, *22*, 1017–1027.

Zhou, C. S., and J. Kurths (2006), Dynamical weights and enhanced synchronization in adaptive complex networks, *Phys. Rev. Lett.*, *96*, 164102.

S. Kravtsov, K. Swanson, and A. A. Tsonis, Department of Mathematical Sciences, Atmospheric Sciences Group, University of Wisconsin-Milwaukee, Milwaukee WI 53201-0413, USA. (aatsonis@uwm.edu)